

Cosmic Microwave Background Anisotropy

Asaf Pe'er¹

March 3, 2017

This part of the course is based on Refs. [1] - [2]. Figures 5-8 are taken from Wayne Hu's CMB tutorial, see <http://background.uchicago.edu/~whu/intermediate/summary.html>

1. Temperature anisotropy

The first observed signal from the expanding universe is the cosmic microwave background (CMB) radiation. This radiation is composed of the photons that were decoupled from the baryons at t_{dec} .

As explained above, density fluctuations present at that time cause fluctuation in the CMB, via (i) coupling to the radiation field, and (ii) their perturbation of the space and time metric. It is widely believed that these same fluctuations in the density grew with time, and eventually resulted in the formation of galaxies and clusters of galaxies (large scale structure LSS). Thus, the observed fluctuations in the CMB are the infant fetus from which galaxies emerge.

Here, I will give a brief description of the CMB fluctuations observed and how they are used to provide the best constraints on the cosmological parameters - Ω , k etc.

A quick note: we avoided the discussion on the **origin** of these fluctuations, as little is known about it. It is believed that they were produced either during the **inflation** epoch or due to some sort of topological defects that existed at some early stage in the evolution of the universe. It is a common practice to assume that these mechanisms produced a **power law** of the form $P(k) \propto k^n$, with some constant spectral index n .

1.1. Observational quantities

The CMB is a major prediction of modern cosmology and of the big bang theory. This is an isotropic radiation at (nearly) constant temperature of 2.7°K , that was discovered by Penzias and Wilson in 1965.

¹Physics Dep., University College Cork

The CMB sky is extremely isotropic, showing similar temperature of 2.72° k in all directions. Only when using a detector with resolution of $\Delta T/T \sim 10^{-3}$, one sees a dipole structure; however, this is attributed to the motion of earth, the sun and the galaxy through the universe.

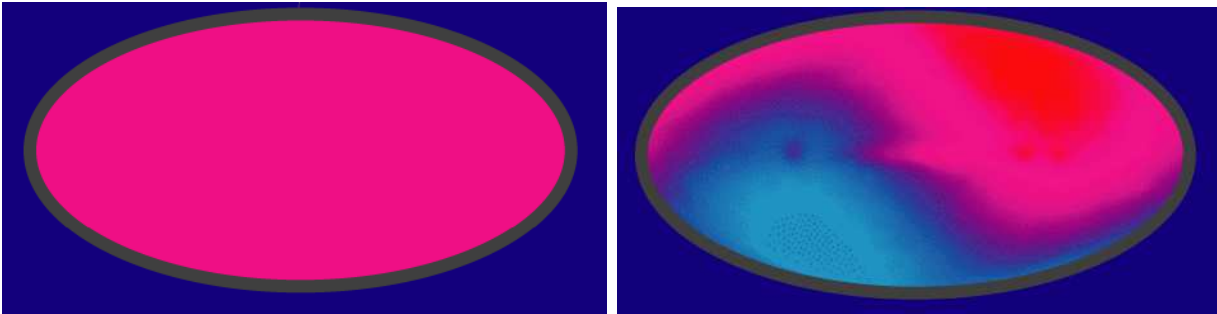


Fig. 1.— Left: The CMB sky is extremely isotropic. Right: only at resolution of $\Delta T/T \sim 10^{-3}$, one sees a dipole structure- however, this is attributed to the motion of earth, the sun and the galaxy through the universe. Data from COBE mission.

As was long predicted and first discovered in 1992 following the launch of the **COBE** mission in 1989, the anisotropy power spectrum of the CMB has a rich structure that can tell us much about the parameters of the cosmological model. Follow-up satellites: WMAP released its data in 2003, and Planck in 2013.

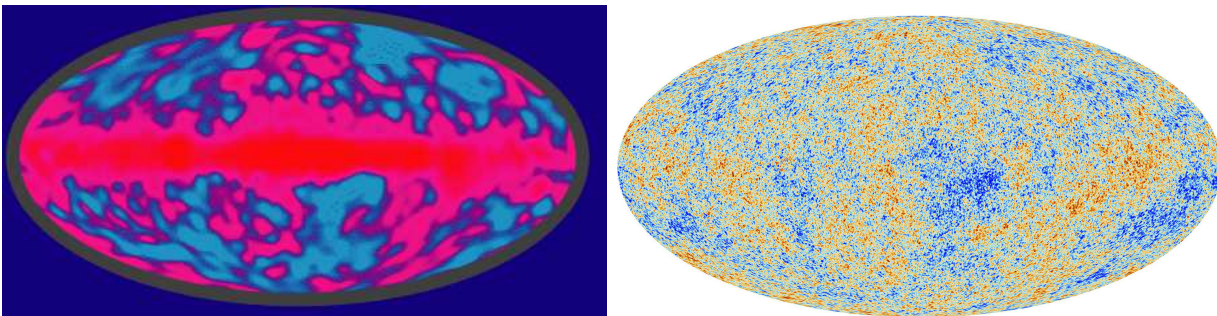


Fig. 2.— Map of the CMB sky, as observed by the COBE (left) and Planck (right) satellites. Fluctuations in the CMB temperature are of the order of $\Delta T/T \approx 7 \times 10^{-5}$. “Cold” spots have temperature of 2.7262° k, while “hot” spots have temperature of 2.7266° k.

Fluctuations in the CMB temperature are quantified by

$$\frac{\Delta T(\hat{n})}{T} \equiv \frac{T(\hat{n}) - \bar{T}}{\bar{T}}, \quad (1)$$

where \bar{T} is the mean temperature and $\hat{n} \equiv (\theta, \phi)$ is a direction on the sky.

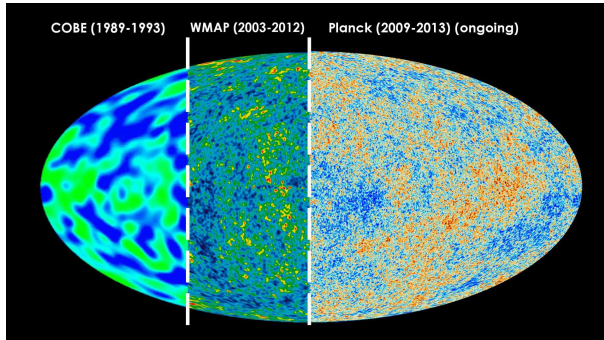


Fig. 3.— Comparison of the resolution of COBE, WMAP and Planck.

Given an all-sky map, we can expand the temperature fluctuations in spherical harmonics:

$$\frac{\Delta T(\hat{n})}{T} = \sum_{l,m} a_{lm} Y_{lm}(\theta, \phi) \quad (2)$$

Note that this is the analogue of a Fourier transform (expansion in plane waves), with a basis that is optimized for describing a distribution on a spherical surface.

The expectation value of the square of the harmonic coefficient, a_{lm} is

$$C_l = \langle |a_{lm}|^2 \rangle \quad (3)$$

Nearly always, though, you will not find plots of C_l , but rather of $l(l+1)C_l$ (possibly normalized to 2π). This is because in EdS cosmology ($\Omega_{m,0} = 1$), for particular type of initial spectrum, known as Harrison-Zel'dovich spectrum, this quantity would be independent on l .

As a rule of thumb, the relation between l and the associated angular scale θ is

$$\theta \sim \frac{\pi}{l} \text{ rad} \sim \frac{180^\circ}{l}. \quad (4)$$

A comoving length $\lambda^{\text{co.}}$ at the last scattering surface (namely, at $z = z_{\text{dec.}}$) subtends to an angle

$$\theta(\lambda^{\text{co.}}) = \frac{\lambda^{\text{co.}}}{d_A(z_{\text{dec.}})(1 + z_{\text{dec.}})} \quad (5)$$

where $d_A(z)$ is the angular diameter (which is defined in the cosmology part of GR). For a given length scale, the corresponding angular scale thus depends on the cosmological parameters: h , $\Omega_{m,0}$ and $\Omega_{\Lambda,0}$.

An important scale is the Hubble radius at decoupling, $r_H = c/H(z_{\text{dec.}})$ (this is similar to the particle horizon at $z_{\text{dec.}}$, except for a factor of order unity). For flat Λ -CDM cosmology, it is

$$\theta_H \sim 0.87^\circ \left(\frac{z_{\text{dec.}}}{1100} \right)^{-1/2}, \quad (6)$$

which corresponds to $l \sim 200$.

On scale larger than θ_H , the observed temperature fluctuations are entirely due to super-horizon perturbations in space and time. These can be decomposed into fluctuations in the energy density of photons, and fluctuation in the gravitational potential (photons lose energy as they climb the potential well). Combined, these are known as **Sachs-Wolfe** effect.

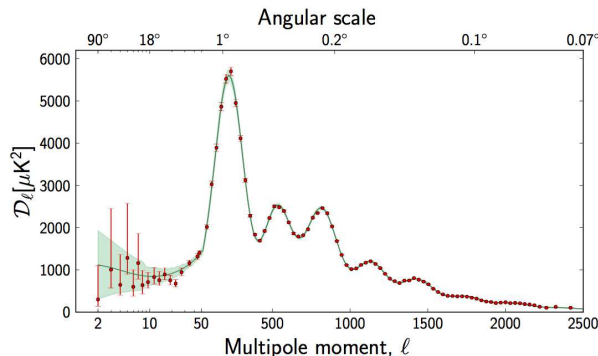


Fig. 4.— Power spectrum of the CMB fluctuations as a function of l reveals clear structure of peaks and decay at large l . The peaks are the acoustic peaks, corresponding to oscillations below the Jeans scale. Their location in l and their relative heights are determined by the cosmological parameters.

2. The acoustic peaks

At smaller angles (larger l) we see several peaks in the power spectrum. As explained above, after entering the horizon, the baryonic perturbations below the Jeans mass start acoustic oscillations. These are driven by the potential perturbations in the dark matter. While denser than average areas gravitationally attract the baryons, pressure from the radiation (which is tightly coupled to the electrons by Thomson scattering) resists gravitational compression, resulting in acoustic oscillations. This situation is analogue to that of mass on a spring, falling under the influence of gravity (see Figure 5).

The resulting sound waves in the photon-baryon fluid create temperature fluctuations. Adiabatic compression of the gas heats it up, while adiabatic expansion of the gas cools

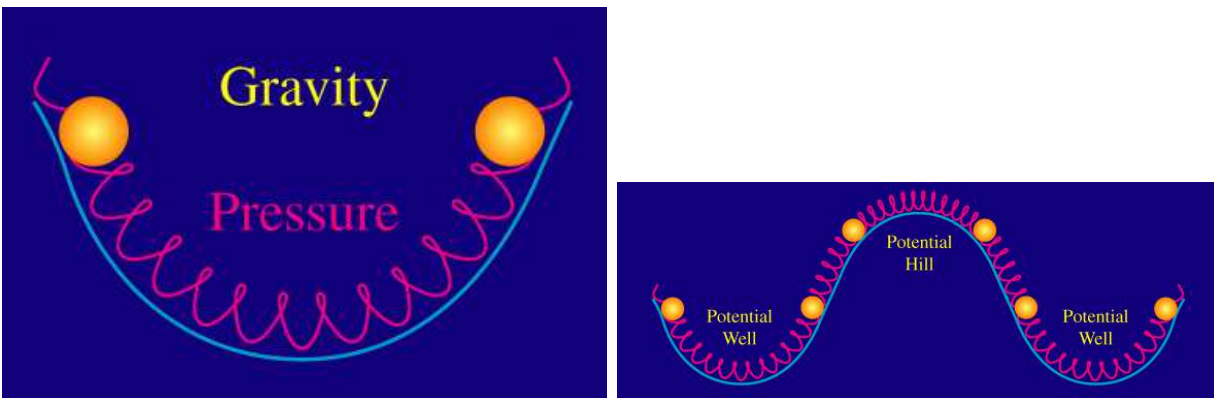


Fig. 5.— Left: acoustic oscillations are analogue to mass oscillating on a spring. Right: fluctuations in the gravitational potential can be thought of as hills and wells into which the baryons fall.

it. These compressions continue as long as the baryons are coupled to the photons, i.e., at $a < a_{\text{dec}}$.

The fluctuations in the potential exist on all scales. As a result, all the modes fluctuates simultaneously, with each mode being independent on the others. As the speed of sound is the same for all modes (and depends on the ratio of baryon to photon energy densities), the modes with the smaller wavelengths oscillate faster.

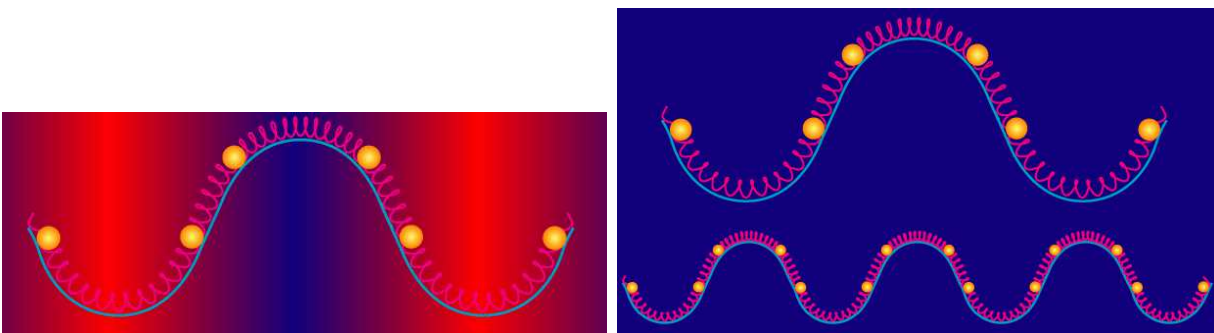


Fig. 6.— Left: in compressed regions, the baryons are slightly hotter. Right: oscillations occur simultaneously on different wavelengths (different modes). The modes with the smaller wavelengths oscillate faster.

At recombination, photons are released, and the pressure of the photon-baryon fluid abruptly drops. Thus, the temperature of photons released is frozen at recombination. In

other words, the last scattering surface produces a snapshot view of the oscillation phases of all the different modes.

The position (in l) of the first acoustic peak is therefore due to the mode that just reached maximal compression in valley / rarefaction on hill top for the first time after recombination. This, in turn, depends on the speed of sound and on the cosmological parameters.

Similarly, the second acoustic peak is due to mode that just reached maximal rarefaction in valley / compression on hill top for the first time after recombination. The wavenumber of the peak are harmonically related to the fundamental scale, which is the scale sound traveled by recombination. Note that since the CMB was released at $z_{\text{dec.}} \approx 1100$, and at that epoch the universe was matter-dominated, the location of the peaks are not sensitive to Ω_λ , but rather to $\Omega_{\text{tot.}} = \Omega_\lambda + \Omega_m$.

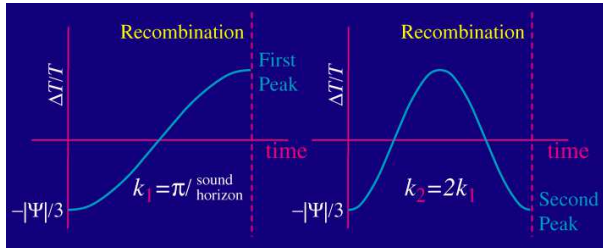


Fig. 7.— The peaks in the CMB fluctuations correspond to those modes that happen to be in extrema at the time of decoupling.

3. Damping on small scales

In addition to Silk damping, we must also consider **diffusion damping**. This damping occurs because the last scattering surface is not exactly a surface, but rather the last scattering surface has some finite width in a (or z). If this width is d , then temperature fluctuations due to modes with a wavelength $\lambda < d$ are washed out. This diffusion damping explains the damping of the CMB power spectrum on small scales.

The typical redshift in which the decoupling take place is $\Delta z \approx 80$. This corresponds to a comoving length scale of ≈ 10 Mpc, corresponding angular scale ~ 0.1 degrees. This leads to suppression of temperature fluctuations on scales $l > 1000$. Silk damping will further reduce fluctuations on scale $l > 2000$.

4. Effect of baryon mass

Increasing density of baryons (relative to that of dark matter) causes stronger compression in valleys - due to the self gravity of the baryons, and less compression on hill-tops.

Since odd peaks (first, third, etc.) correspond to compression in valleys, whereas even peaks (second, fourth, etc.) correspond to compression on hill tops, the baryon to dark matter ratio controls the ratio of odd to even peak heights. These fits thus provide a direct probe of the ratio of DM to baryons, which is roughly 6:1.

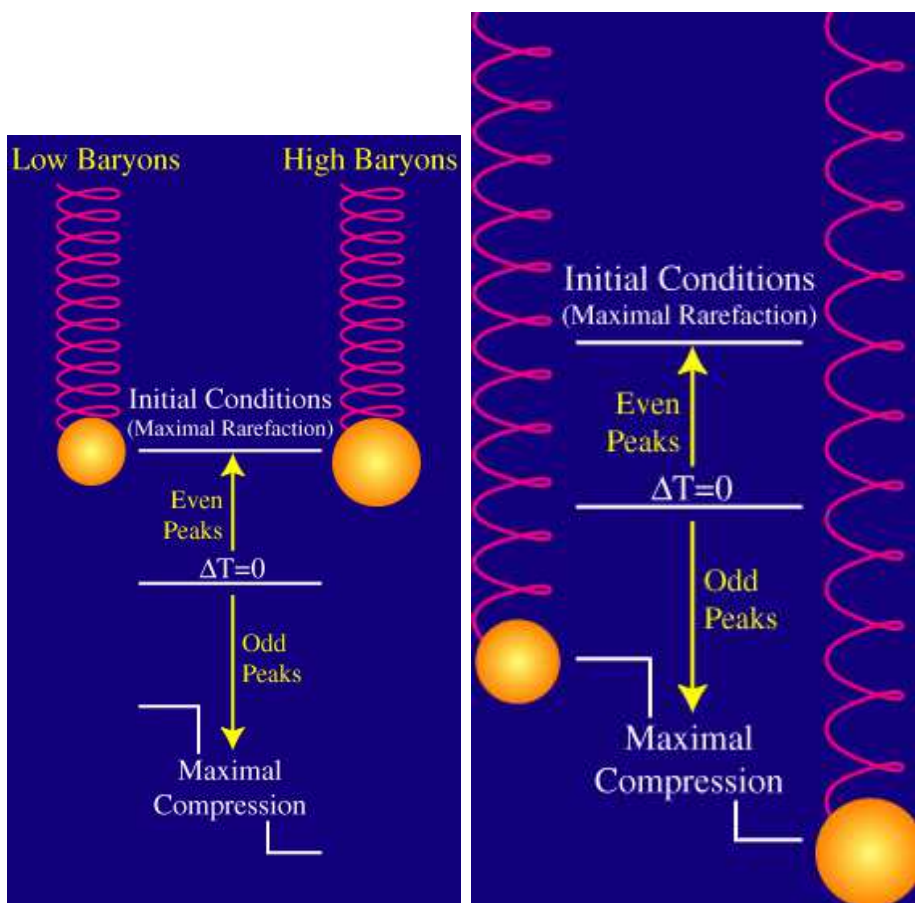


Fig. 8.— Increasing baryon density (relative to that of dark matter) causes stronger compression in valleys and less compression on hilltops. This will be manifested in the odd-to-even peak heights.

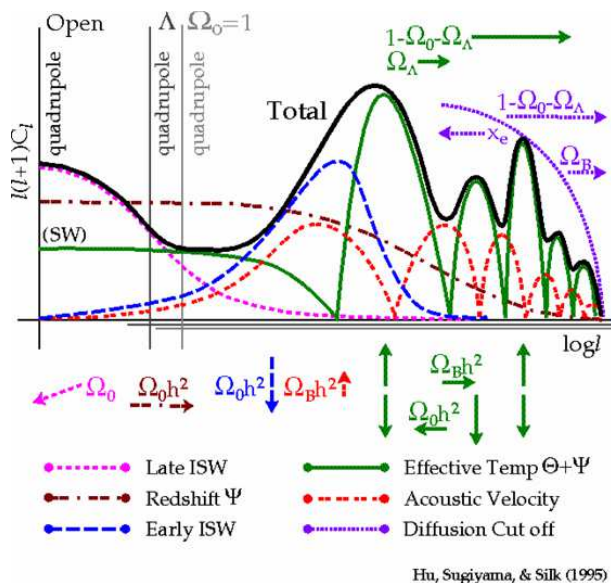


Fig. 9.— Dependence of peak location and strength on cosmological model parameters

REFERENCES

- [1] H. Mo, F. van den Bosch and S. White, *Galaxy Formation and Evolution* (Cambridge), chapter 6.
- [2] T. Padmanabhan, *Structure Formation in the Universe* (Cambridge), chapter 6.